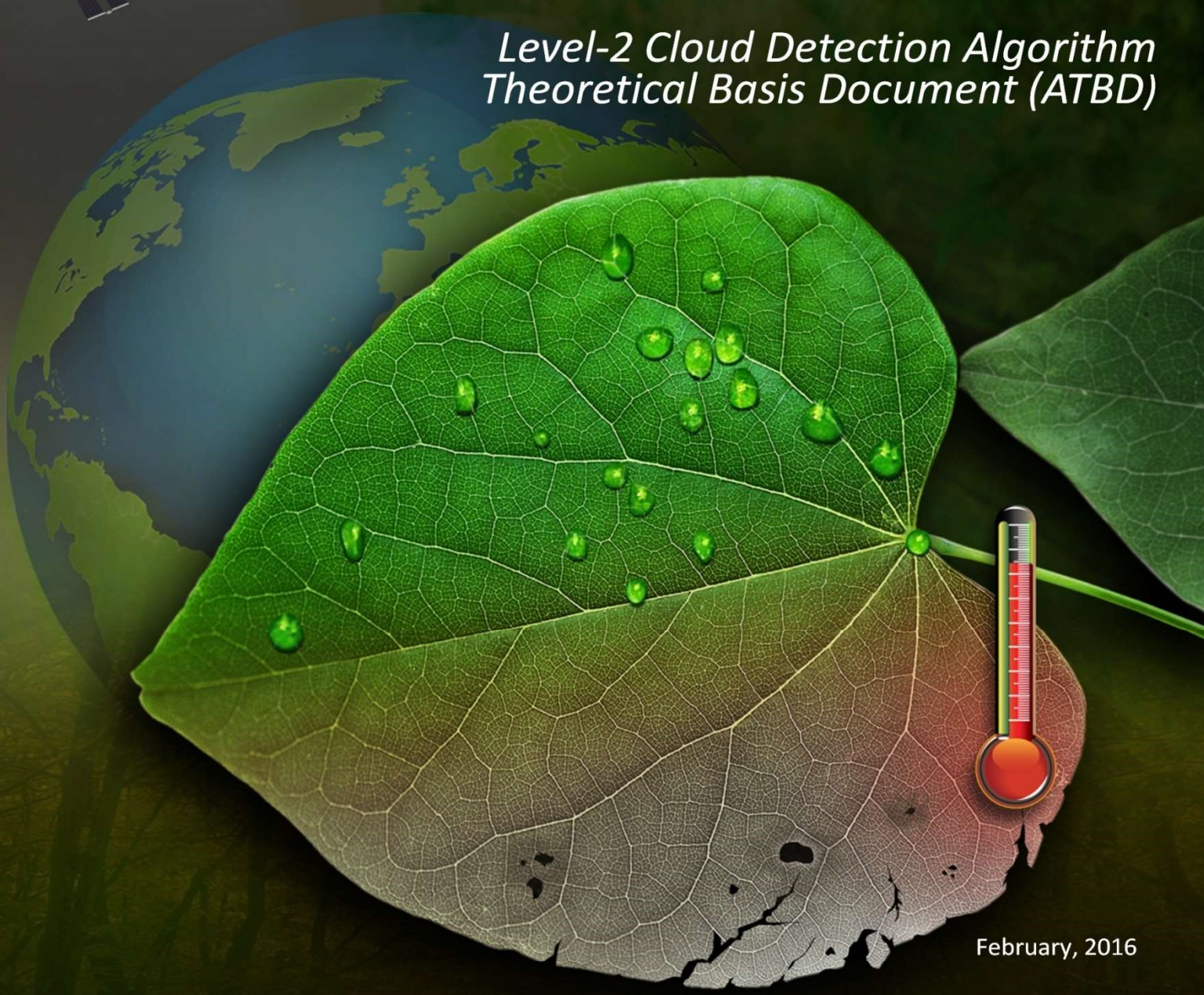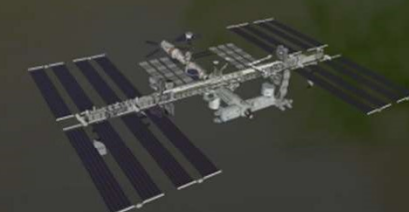# ECOSTRESS

ECOsystem Spaceborne Thermal Radiometer Experiment on Space Station

Level-2 Cloud Detection Algorithm Theoretical Basis Document (ATBD)

February, 2016

Glynn C. Hulley
Co-Investigator
Jet Propulsion Laboratory
California Institute of Technology

Simon J. Hook
Principal Investigator
Jet Propulsion Laboratory
California Institute of Technology

Change History Log

Revision	Effective Date	Prepared by	Description of Changes
Draft	02/23/2016	Glynn Hulley	ECOSTRESS L2 CLOUD ATBD first draft. Approved for public release, JPL D-94644
Version 1	02/23/2018	Glynn Hulley	Updates to cloud tests employed, output product SDS details, simulated ECOSTRESS images and cloud tests using VIIRS thermal data.
Version 2	10/06/2022	Glynn Hulley	Updates for new Collection 2 algorithm and product

Contacts

Readers seeking additional information about this study may contact the following:

Glynn C. Hulley

MS 183-501
Jet Propulsion Laboratory
4800 Oak Grove Dr.
Pasadena, CA 91109
Email: *glynn.hulley@jpl.nasa.gov*
Office: (818) 354-2979

ECOSTRESS Science Team

Principal Investigator:

Simon Hook, Jet Propulsion Laboratory

Co-Investigators:

Glynn Hulley, JPL

Joshua Fisher, JPL

Rick Allen, University of Idaho

Martha Anderson, USDA

Andrew French, USDA

Eric Wood, Princeton University

Collaborators:

Christopher Hain, University of Maryland

Abstract

The ECOsystem Spaceborne Thermal Radiometer Experiment on Space Station (ECOSTRESS) mission was selected as a NASA Earth-Ventures Instrument (EV-I) Class-D mission on the International Space Station (ISS). ECOSTRESS will answer science questions related to water use and availability in several key biomes of the terrestrial biosphere using temperature information derived from the thermal infrared (TIR) measurement. The inclined, precessing ISS orbit will enable ECOSTRESS to sample the diurnal cycle in critical regions across the globe at spatiotemporal scales unexploited by current instruments in Sun-synchronous polar and high-altitude geostationary orbits. The instrument includes a TIR multispectral scanner with five spectral bands in the TIR between 8 and 12.5 µm, and leverages off the functionally-tested Prototype ECOSTRESS Thermal Infrared Radiometer (PHyTIR) space-ready hardware developed under the NASA Instrument Incubator Program. The five bands have a NEΔT of <0.1 K at 300K and all bands have a spatial scale of 38m x 68m with a swath width of 402 km (53°). The two primary Level-2 products that will be generated by ECOSTRESS TIR data are the land surface temperature (LST) and emissivity. A critical aspect of minimizing uncertainties in these products and higher level products (L3, L4) is an accurate and reliable cloud detection and masking algorithm. This document describes the methodology behind developing the ECOSTRESS L2 Cloud Mask Algorithm (ECOCLOUD), and challenges associated with cloud detection.

Contents

Figures

Tables

1   Introduction

The ECOsystem Spaceborne Thermal Radiometer Experiment on Space Station (ECOSTRESS) mission consists of a thermal infrared (TIR) multispectral scanner with one shortwave infrared (SWIR) band at 1.6 µm, and five spectral bands operating between 8 and 12.5 µm. The data in these six bands will be acquired at a spatial resolution of 38m x 68m with a swath width of 402 km (53°) from the nominal International Space Station (ISS) altitude of 400 +/- 25 km.

This document outlines the theory and methodology for generating the ECOSTRESS Level-2 Cloud Mask product in Collection 2 using a statistical-based single-band thresholding approach with clear-sky brightness temperature look up tables. In Collection 1, two cloud detection tests were employed using bands 4 and 5 with fixed day and night thresholds, however this yielded unsatisfactory results since ECOSTRESS observations occur at all hours of the day. In Collection 2, the thresholds are dynamically interpolated based on time of day, month of year, and location to take into account changes in the land surface emissivity.

Discriminating clouds is a challenging endeavor and depends on not only the type of cloud being detected, but also the type of surface over which the cloud is detected. Clouds are brighter and colder than the land surface they obscure and these properties can be exploited with the ECOSTRESS high spatial resolution TIR bands. Cloud and land surface variability, however, creates ambiguity in cloud screening. A cloud signature that works well for one scene may be ineffective for another, depending on the land surface type. Accurate cloud identification is also affected by surface features such as snow, ice, and reflective sand that have reflectance signatures similar and in some cases identical to clouds in the visible bands, especially at higher elevations. For these reasons, the ECOSTRESS cloud mask includes a confidence level mask

that classifies pixels as follows (0 = confident cloudy, 1 = probably cloudy, 2 = probably clear, and 3 = confident clear).

ECOSTRESS will address critical questions on plant–water dynamics and future ecosystem changes with climate through an optimal combination of TIR measurements with high spatiotemporal and spectral resolution from the ISS. ECOSTRESS will fill a key gap in our observing capability, advance core NASA and societal objectives, and allow us to address the following science objectives: 1. Identify critical thresholds of water use and water stress in key climate sensitive biomes; 2. Detect the timing, location, and predictive factors leading to plant water uptake decline and/or cessation over the diurnal cycle; and, 3. Measure agricultural water consumptive use over the contiguous United States (CONUS) at spatiotemporal scales applicable to improve drought estimation accuracy.

These questions will be answered using the ECOSTRESS Level-3 products; Evapotranspiration (ET), Water Use Efficiency (WUE), and Evaporative Stress Index (ESI). The LST, which can be retrieved remotely from thermal infrared (TIR; 8-12.5 μm) retrievals is a necessary input to energy balance models that derive ET (Allen et al. 2007; Anderson et al. 2011; Fisher et al. 2008). Currently, there is no single satellite sensor or constellation of sensors that provide TIR data with sufficient spatial, temporal, and spectral resolution to reliably estimate ET at the global to local scale over the diurnal cycle. Measurements are either too coarse (e.g., MODIS, GOES: >1-km resolution) or infrequent (e.g., Landsat: 16-day revisit). Table 1 gives details of measurement characteristics of ECOSTRESS compared to current and future TIR missions.

Table 1: ECOSTRESS measurement characteristics as compared to other spaceborne TIR instruments.

Instrument	Platform	Resolution (m)	Revisit (days)	Daytime overpass	TIR bands (8-12.5 μm)	Launch year
ECOSTRESS	ISS	38 × 68	3-5	Multiple	5	2018
ECOSTRESS	TBD	60	5	10:30 am	7	2024
ASTER	Terra	90	16	10:30 am	5	1999
ETM+/TIRS	Landsat 7/8	60-100	16	10:11 am	1/2	1999/2013
VIIRS	Suomi-NPP	750	Daily	1:30 am/pm	4	2011
MODIS	Terra/Aqua	1000	Daily	10:30/1:30 am/pm	3	1999/2002
GOES	Multiple	4000	Daily	Every 15 min	2	2000

The remainder of the document will discuss the ECOSTRESS instrument characteristics,

provide a background on cloud detection algorithms, and show some examples of the

ECOCLOUD algorithm.

2 ECOSTRESS Instrument Characteristics

The ECOSTRESS instrument will be implemented by placing the existing space-ready Prototype ECOSTRESS Thermal Infrared Radiometer (PHyTIR) on the ISS and using it to gather the measurements needed to address the science goals and objectives. PHyTIR was developed under the NASA Earth Science Technology Office (ESTO) Instrument Incubator Program (IIP).

The TIR instrument will acquire data from the ISS with a 38-m in-track by 68-m cross-track spatial resolution in five spectral bands, located in the TIR part of the electromagnetic spectrum between 8 and 12.5 μm shown in Figure 1. The center position and width of each band is provided in Table 2. The positions of three of the TIR bands closely match the first three thermal bands of ASTER, while two of the TIR bands match bands of ASTER and MODIS typically used for split-window type applications (ASTER bands 12–14 and MODIS bands 31, 32). It is expected that small adjustments to the band positions will be made based on ongoing engineering filter performance capabilities.
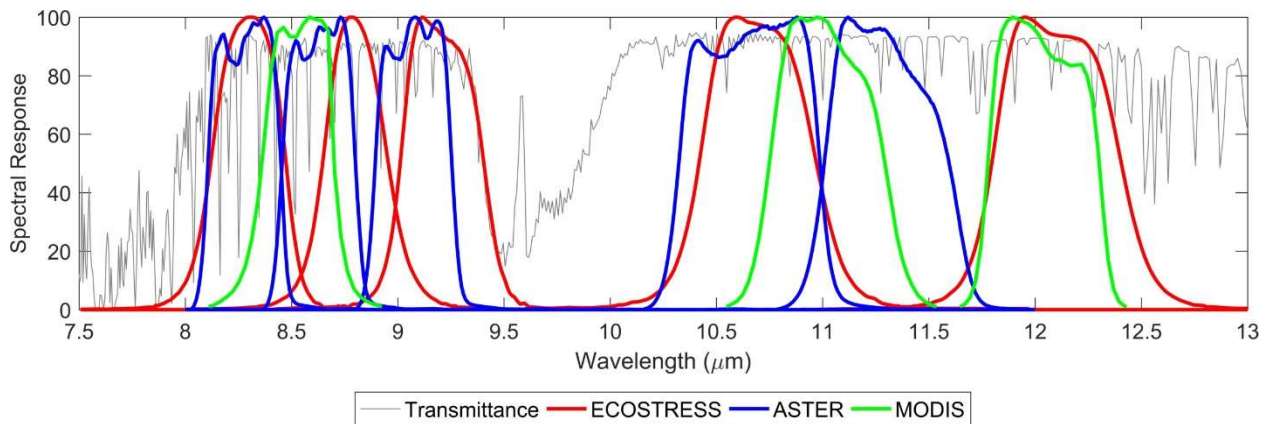
Figure 1: ECOSTRESS TIR instrument spectral bands from 8-12.5 micron (red) compared to ASTER (blue) and MODIS (green) with a typical atmospheric transmittance spectrum in black highlighting the atmospheric window regions.
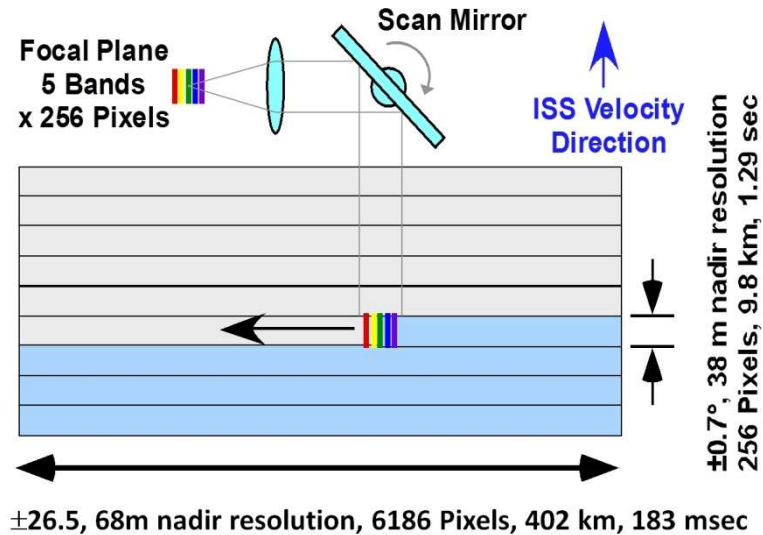
Figure 2: ECOSTRESS TIR scanning scheme

The TIR instrument will operate as a push-whisk mapper, similar to MODIS but with 256 pixels in the cross-whisk direction for each spectral channel (Figure 2), which enables a wide swath and high spatial resolution. As the ISS moves forward, the scan mirror sweeps the focal plane ground projection in the cross-track direction. Each sweep is 256-pixels wide. The different spectral bands are swept across a given point on the ground sequentially. From the 400±25-km ISS altitude, the resulting swath is 402 km wide. A wide continuous swath is produced even with an ISS yaw of up to ±18.5°.A conceptual layout for the instrument is shown in Figure 3. The scan mirror rotates at a constant angular speed. It sweeps the focal plane image 53° across nadir, then to two on-board blackbody targets at 300 K and 340 K. Both blackbodies will be viewed with each cross-track sweep every 1.29 seconds to provide gain and offset calibrations.

2.1   Radiometer

The radiometer was designed and built by experienced flight hardware engineers with flight in mind. Preliminary structural analysis indicates that, with a change of the yoke material
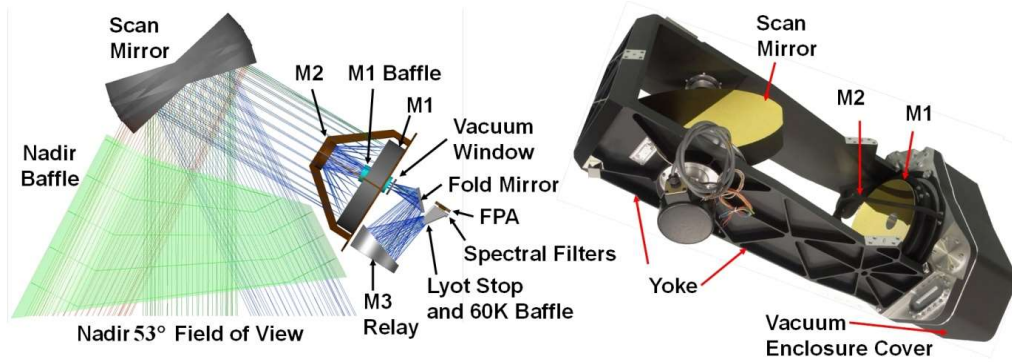
Figure 3: ECOSTRESS TIR conceptual layout

from 6061 to 7075 aluminum, the radiometer structure will have the necessary margins to withstand launch loads. Phase A-B will include a full structural analysis. The Thales LPT9310 cryocoolers will be replaced to change the welded tubing length connecting the compressors to the expanders. Also, the existing spectral filter assembly with three filters will be replaced with a new assembly containing the five filters. All replacements are straightforward, requiring only disassembly and reassembly, using standard flight procedures and documentation.

2.2   Optics

The f/2 optics design is all reflective, with gold-coated mirrors. The 60-K focal plane will be single-bandgap mercury cadmium telluride (HgCdTe) detector, hybridized to a CMOS readout chip, with a butcher block spectral filter assembly over the detectors. Thirty-two analog output lines, each operating at 10–12.5 MHz, will move the data to analog-to-digital converters. All the TIR channels are quantized at 14 bits. Expected sensitivities of the five channels, expressed in terms on noise-equivalent temperature difference, are shown in Figures 4 and 5. The TIR instrument will have a swath width of 402 km (53°) with a pixel spatial resolution of 38m x 68 m and it will acquire data over key climate sensitive biomes including tropical/dry transition forests and boreal forests. The large swath width of the TIR instrument combined with the

inclined, precessing ISS orbit will enable ECOSTRESS to sample at varying times throughout the day over the course of a year. Figure 6 shows an example at 50° latitude.
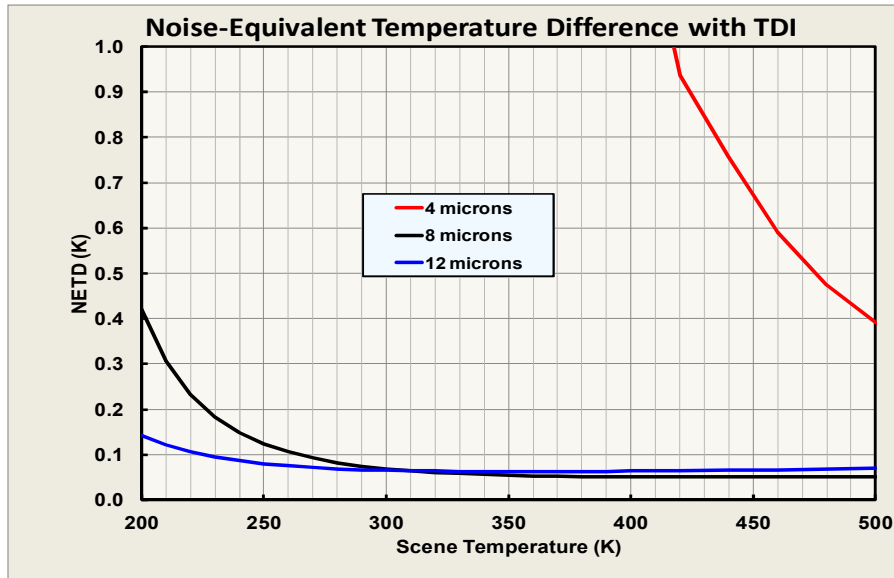
Figure 4: ECOSTRESS TIR predicted sensitivity 200–500 K.
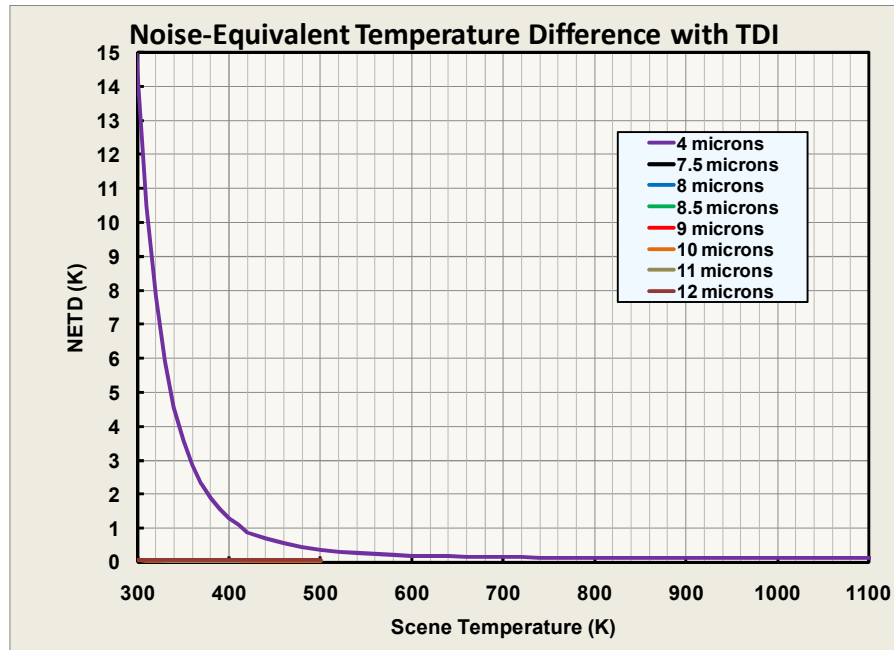
Figure 5: ECOSTRESS TIR predicted sensitivity 300–1100 K.
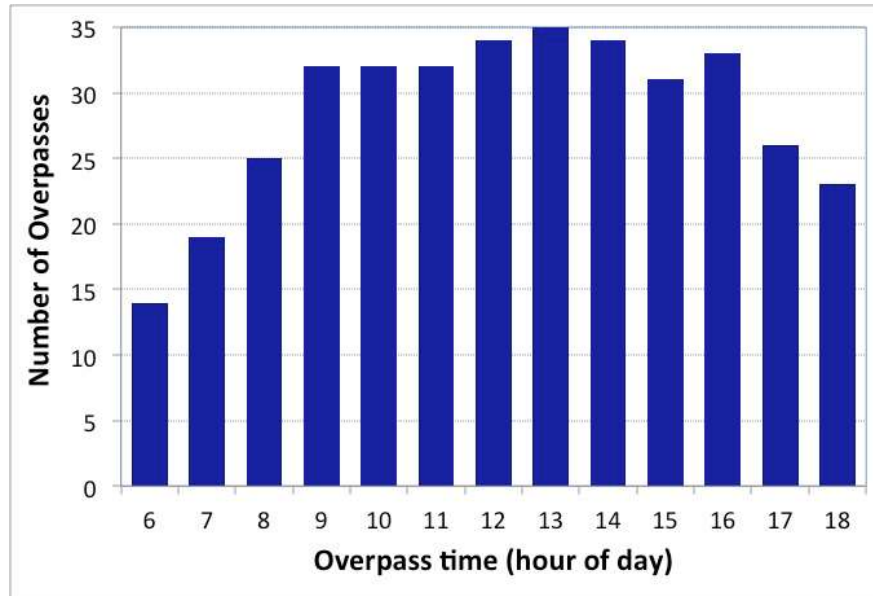
Figure 6: ECOSTRESS number of overpasses versus overpass time at 50° latitude.

Table 2: ECOSTRESS TIR Instrument and Measurement Characteristics

Spectral	
Bands (µm)	8.28, 8.63, 9.07, 11.35, 12.05
Bandwidth (µm)	0.34, 0.35, 0.36, 0.54, 0.54
Accuracy at 300 K	<0.01 µm
Radiometric	
Range	Bands 1–5 = 200 K – 500 K;
Resolution	< 0.05 K, linear quantization to 14 bits
Accuracy	< 0.5 K 3-sigma at 250 K
Precision (NEdT)	< 0.1 K
Linearity	>99% characterized to 0.1 %
Spatial	
IFOV	38 m in-track, 68 m cross-track
MTF	>0.65 at FNy
Scan Type	Push-Whisk
Swath Width at 400-km altitude	402 km (+/- 26.5°)
Cross Track Samples	6,186
Swath Length	9.8 km (1.29 sec)
Down Track Samples	256
Band to Band Co-Registration	0.2 pixels (12 m)
Pointing Knowledge	10 arcsec (0.5 pixels) (approximate value, currently under evaluation)
Temporal	
Orbit Crossing	Multiple
Global Land Repeat	Multiple
On Orbit Calibration	
Lunar views	1 per month
Blackbody views	1 per scan
Deep Space views	1 per scan
Surface Cal Experiments	2 (day/night) every 5 days
Spectral Surface Cal Experiments	1 per year
Data Collection	
Time Coverage	Day and Night
Land Coverage	Land surface above sea level
Water Coverage	n/a
Open Ocean	n/a
Compression	2:1 lossless

3 Science Objectives

ECOSTRESS will address critical questions on plant–water dynamics and future ecosystem changes with climate through an optimal combination of TIR measurements with high spatiotemporal resolution (38 × 68 m; every few days at varying times of day), and spectral resolution (5 spectral bands) from the International Space Station (ISS). The overarching goal of the ECOSTRESS is to measure water use and water stress across natural and managed ecosystems to understand vegetation change under limiting water conditions. This overarching goal will be answered by three broad questions;

> ➢ How is the terrestrial biosphere responding to changes in water availability?
>
> ➢ How do changes in diurnal vegetation water stress impact the global carbon cycle?
>
> ➢ Can agricultural vulnerability be reduced through advanced monitoring of agricultural water consumptive use and improved drought estimation?

To address these science questions, three primary objectives have been identified:

1. Identify critical thresholds of water use and water stress in key climate sensitive biomes;

2. Detect the timing, location, and predictive factors leading to plant water uptake decline and/or cessation over the diurnal cycle; and,

3. Measure agricultural water consumptive use over the contiguous United States (CONUS) at spatiotemporal scales applicable to improve drought estimation accuracy.

These science questions and objectives combine to form three core science hypotheses:

• **H1**: The WUE of a climate hotspot is significantly lower than non-hotspots of the same biome type;

• **H2**: Daily ET is overestimated when extrapolating from morning-only observations; and

• **H3**: Remotely sensed ET measured at the field scale will improve drought prediction over managed ecosystems.

4   Theory and Methodology

4.1   Objectives

The cloud mask from ECOCLOUD will indicate whether a given view of the earth surface is unobstructed by clouds. The cloud mask will be generated at 70-m spatial resolution. Input to the ECOCLOUD algorithm is assumed to be calibrated and geolocated L1B TIR brightness temperature data. The cloud mask will be determined for good data only (i.e., fields of view where data in ECOSTRESS TIR bands have radiometric integrity). Several points need to be made regarding the approach to the ECOSTRESS cloud mask presented in this Algorithm Theoretical Basis Document (ATBD).

(1) The cloud mask confidence level flags will be distributed as a separate additional L2 product, which investigators can use to screen data as appropriate for their studies, however a final cloud mask will be included with the L2 LST&E product for users who wish to use the standard confidence levels (cloud = confident + probably cloudy pixels).

(2) The cloud mask ATBD assumes that calibrated, quality controlled TIR data are the input and a cloud mask is the output.

(3) In certain heavy aerosol loading situations (e.g., dust storms, volcanic eruptions, and forest fires) the cloud mask may flag the aerosol-laden atmosphere as cloudy.

The cloud mask products will include a confidence level mask (0 = confident cloudy, 1 = probably cloudy, 2 = probably clear, and 3 = confident clear) and a final cloud mask (1 = cloud, 0 = clear) based on a combination of the confidence flags and digital elevation model (see Table 4). In summary, our approach to the ECOSTRESS cloud mask is, in its simplest form, to provide a binary confidence level output for each pixel, and a final cloud mask based on standard processing approach.

4.2   Background

The ECOSTRESS cloud mask in Collection 2 uses a similar method as the dynamic

threshold (or Bayesian classification scheme) used for the Advanced Along Track Scanning

Radiometer (AATSR) (Bulgin et al. 2014; Merchant et al. 2014), and its successor the Sea and

Land Surface Temperature Radiometer (SLSTR). The algorithm derives the pixel-level cloud

mask using a combination of TIR simulated clear-sky brightness temperatures that are

interpolated from Look Up Tables (LUT) onto the satellite scene, and is valid both day and night.

4.3   Brightness temperature calculation

Theoretically, brightness temperatures for each ECOSTRESS band can be calculated on a

pixel-by-pixel basis by inverting the Planck equation:

$$T_b(\lambda) = \frac{c2}{\lambda \cdot \ln\left(\frac{c1}{\lambda^5 \cdot \pi \cdot L_\lambda} + 1\right)} \tag{1}$$

where: λ is wavelength in μm, $c1 = 0.0143877$, $c2 = 3.741775\text{e-}22$, L_λ is the at-sensor spectral

radiance in $W/(m^2 \cdot sr \cdot \mu m)$

However, this formulation will increasingly become inaccurate for a sensor's spectral

response that deviates from delta function behavior. Instead, we use a look up table (LUT)

approach in which the Planck function is used to compute expected radiances for each respective

ECOSTRESS band's spectral response functions over a range of temperatures in 0.01 K intervals

that encompass the full range of expected Earth-like temperatures (typically 150 to 380 K). This

results in a table of values of radiances versus temperatures for each given sensor. The table can

then simply be 'inverted' by interpolating to get the desired temperature. The table can be

modified to any desired precision by decreasing the step size interval (e.g. from 0.01 to 0.001 K).

5 Cloud mask implementation

5.1 Brightness temperature LUT interpolation and thresholding

The expected clear-sky brightness temperatures are simulated using forward calculations

from the RTTOV-12 radiative transfer model with input atmospheric profile information from

the GEOS5-FP product (GMAO) on 0.25×0.25° grids combined with surface emissivity from the

Combined ASTER MODIS Emissivity for Land (CAMEL) v2 product (Borbas et al. 2018; Feltz

et al. 2018). For each month of simulations and for each 6hr period, a statistical distribution of

the clear-sky brightness temperatures for each grid cell location is used to determine the three

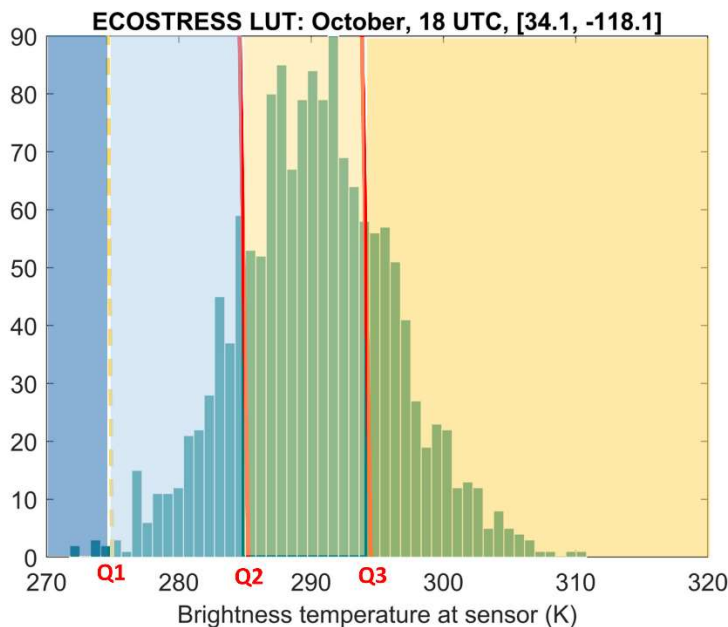confidence level thresholds (Q1, Q2, Q3) using an interquartile range (IQR) approach (Figure 7).

Figure 7: ECOSTRESS clear-sky brightness temperature (BT) distribution for the month of October at 18 UTC for location 34.1 N, -118.1 (JPL, Pasadena). Cloud confidence levels are determined from thresholds set at Q1, Q2 and Q3 (see text for details).
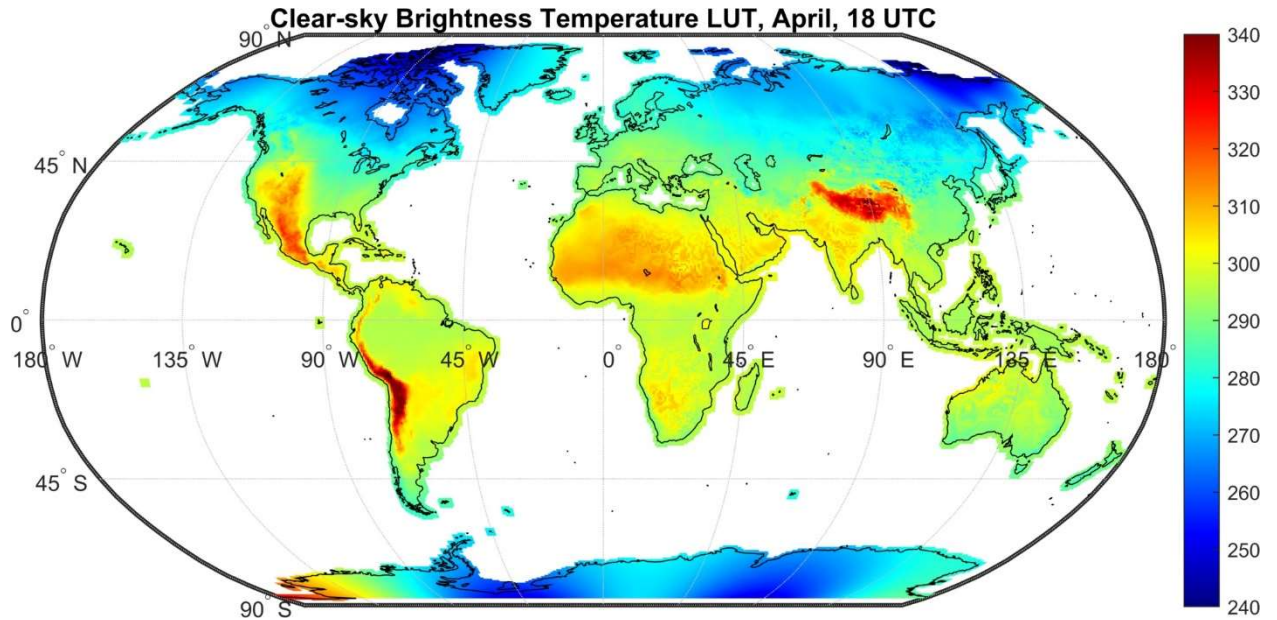
Figure 8: ECOSTRESS clear-sky brightness temperature (BT) climatology Look Up Table (LUT) for April at 18 UTC. ECOSTRESS observed BT's during April at or near 18 UTC that fall below these values are considered cloudy.

The first confidence level is determined by Q1 and is used to find confident cloudy pixels:

$$Q1 = Q2 - 1.5 \times IQR$$

Where $IQR = Q3 - Q2$, Q2 is the 25th percentile and Q3 is the 75th percentile. Then any pixels with brightness temperatures less than Q1 are considered to be confident cloudy pixels. The second confidence level, probably cloudy pixels, is determined as pixels with brightness temperatures falling between Q1 and Q2. The third confidence level, probably clear pixels falls between Q2 and Q3 and lastly the fourth confidence level, confident cloudy pixels, are pixels with brightness temperatures greater than Q3.

Implementation of the cloud mask involves interpolating the global clear-sky brightness temperature Look Up Table (LUT) (see Figure 7) for each confidence level onto each ECOSTRESS scene using bilinear interpolation between surrounding GEOS5 grid points and a temporal interpolation between the 6-hourly analysis fields. Figure 8 shows an example of a global gridded LUT for the month of August at 18 UTC. Note that the thresholds are determined

for ocean along coastal zones as well, with a 2 degree (~200 km) buffer along coastlines. For ECOSTRESS observations over open ocean, the coastal values are extrapolated into open ocean. While this may introduce uncertainty, the primary science focus of ECOSTRESS data is over land.

Figure 9 shows an example of interpolation of the global grid LUT onto an ECOSTRESS scene on 5 April, 2022 at 18:46 UTC consisting of cloud over high elevation areas in the Rocky Mountains, USA. Cloud over high elevation areas is a challenging condition due to varying lapse rates and the presence of snow/ice during wintertime. To refine the thresholds further over these regions, we adjust the LUT thresholds using a standard lapse rate of 6.5 K/km using the ECOSTRESS DEM included in the Geolocation product for the elevation. For this particular case, pixels with observed brightness temperatures less than the LUT values are considered confident cloudy, since the LUT shown here represents the Q1 confident cloudy threshold.
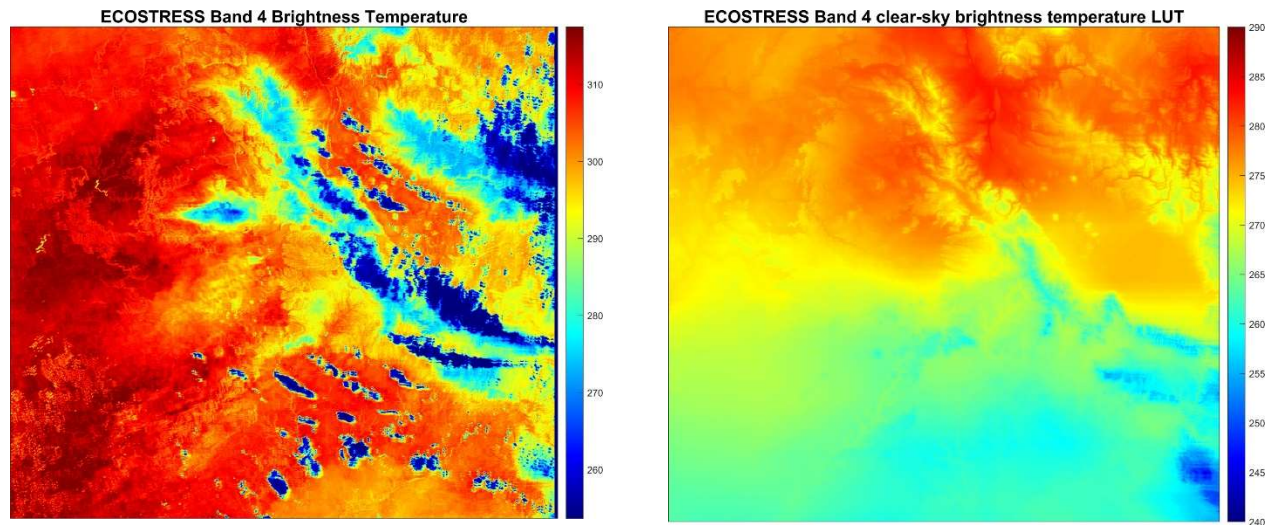

Figure 9: ECOSTRESS example of observed brightness temperature (BT) in band 4 (left) and spatially and temporally interpolated BT LUT (for Q1 confidence threshold) onto the ECOSTRESS scene on 5 April, 2022 at 18:46 UTC.

5.2 Cloud mask confidence flags

The cloud product will contain two masks, a cloud confidence mask, and final estimated cloud mask. Users can interpret these data sets as follows:

1. Cloud_confidence contains the results of the brightness temperature LUT test with confidence levels set according to three threshold levels described above

    a. 0 = confident clear

    b. 1 = probably clear

    c. 2 = probably cloudy

    d. 3 = confident cloudy

2. Cloud_final contains a final cloud mask (1=cloud, 0=clear) based on the following criteria:

    a. For elevations < 2km, cloud = probably cloud + confident cloudy pixels

    b. For elevations >2km, cloud = confident cloudy pixels

Users can interpret the confidence levels and estimation of the final cloud mask as they wish, but the generalized rationale for the above logic is that mountainous areas with higher elevation will have larger uncertainties in the cloud mask due to the presence of snow/ice and effects of shading and varying temperature lapse rates. As a result only confident cloudy pixels are classified as cloud. For low lying regions using both probably and confident cloudy pixels provided a good balance between false positive and false negative cloud errors. If the user has zero tolerance for any nearby or possible cloud, then only confident clear pixels should be used, similarly if some cloud can be tolerated, then only confident cloudy pixels should be used.

Figure 10 and 11 show results of the Cloud_confidence and Cloud_final masks for an ECOSTRESS scene shown in Figure 9. Note that areas classified as probably cloud in the confidence mask are likely clear areas at higher elevations. For this reason, only the confident cloudy mask should be used to screen for cloud pixels. These thresholds are set so that in snow/ice conditions only confident cloudy pixels should be trusted as being cloud. The final cloud mask in Figure 11 is based on criteria 2b above, and the presence of cloudy pixels shows high correlation with the coldest brightness temperatures (likely cloud) in Figure 9.
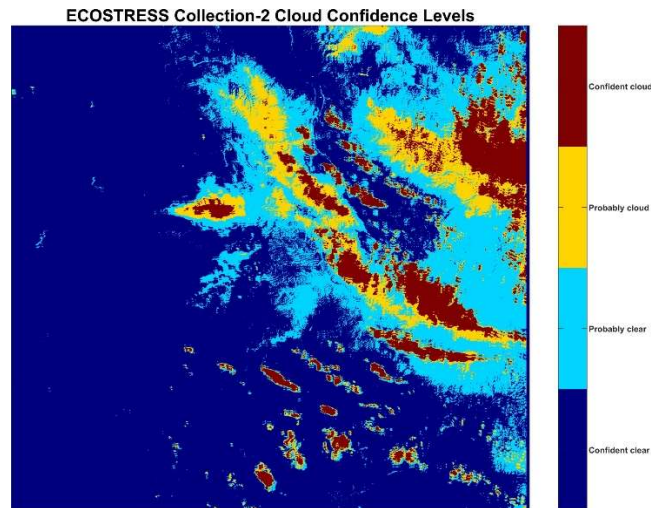

Figure 10: ECOSTRESS cloud confidence flag for a scene on 5 April, 2022 at 18:46 UTC.
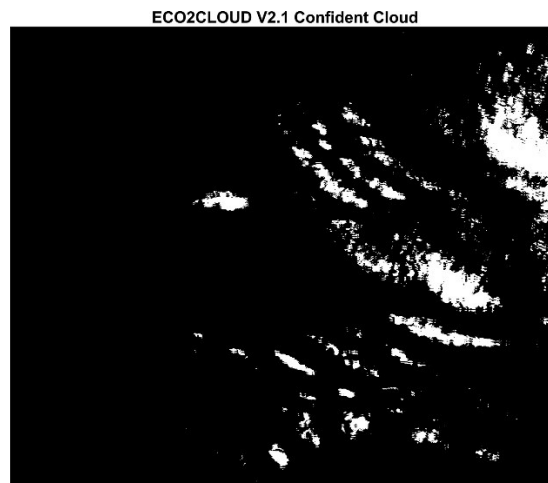
Figure 11: ECOSTRESS final cloud mask for a scene on 5 April, 2022 at 18:46 UTC.

Figure 12: Further examples of the ECO2CLOUD v2.1 product (right) compared to ECOSTRESS band 4 brightness temperatures (left, cloud = cooler temps, blues and greens) for a wide variety of different types of scenes: (top) a very hot scene over Central valley with cooler coastal region, (middle) a very cold scene over Chesapeake bay during winter, and (bottom) a scene with mostly ocean surrounding Kuai, Hawaii.

6 Scientific Data Set (SDS) Variables

The ECOSTRESS L2 Cloud Mask product will be archived in Hierarchical Data Format 5 - Earth Observing System (HDF5-EOS) format f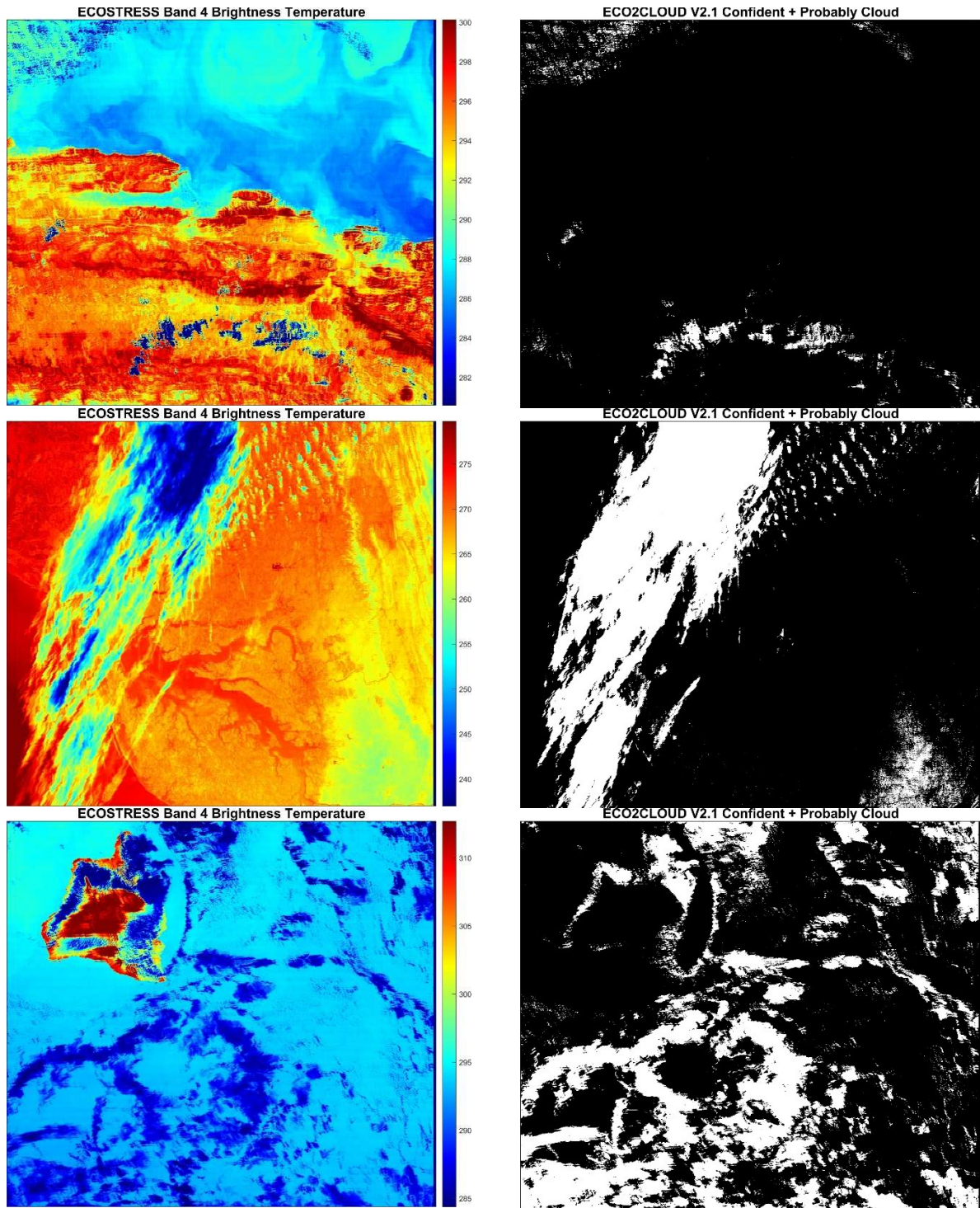iles. HDF is the standard archive format for NASA EOS Data Information System (EOSDIS) products. The L2 Cloud files will contain global attributes described in the metadata, and scientific data sets (SDSs) with local attributes. Unique in HDF-EOS data files is the use of HDF features to create point, swath, and grid structures to support geolocation of data. These structures (Vgroups and Vdata) provide geolocation relationships between data in an SDS and geographic coordinates (latitude and longitude or map projections) to support mapping the data. Attributes (metadata), global and local, provide various information about the data. Users unfamiliar with HDF and HDF-EOS formats may wish to consult Web sites listed in the Related Web Sites section for more information.

Table 7 details the data sets included in the L2_CLOUD output. Users can interpret the data sets as follows:

1. Cloud_confidence contains the results of the brightness temperature LUT test with confidence levels set according to different threshold levels: 0 = confident clear, 1 = probably clear, 2 = probably cloudy, and 3 = confident cloudy.

2. Cloud_final contains a final cloud mask (1=cloud, 0=clear) based on the following criteria:

   c. For elevations < 2km, cloud = probably cloud + confident cloudy pixels

   d. For elevations >2km, cloud = confident cloudy pixels

6.1   Scientific Data Sets (SDS)

Table **3**. The SDSs in the ECOSTRESS L2 Cloud product.

SDS	Long Name	Data type	Units	Valid Range	Fill Value	Scale Factor	Offset
Cloud_confidence	Brightness temperature LUT test	uint8	3=confident cloudy 2=probably cloudy 1=probably clear 0=confident clear	0-3	255	1	0
Cloud_final	Final cloud mask	uint8	1=cloud 0=clear	0-1	255	1	0

6.2   Attributes

Table **4**. The metadata definition in the ECOSTRESS L2 Cloud product.

Name	Type	Size	Example
Group	**L2 CLOUD Metadata**		
QAPercentCloudCover	Int	4	80
CloudMeanTemperature	LongFloat	8	231
CloudMaxTemperature	LongFloat	8	275
CloudMinTemperature	LongFloat	8	221
CloudSDevTemperature	LongFloat	8	0.45

7   References

Ackerman, S., Strabala, K.I., Menzel, P., Frey, R., Moeller, C.C., Gumley, L.E., Baum, B., Seemann, S.W., & Zhang, H. (2006). Discriminating clear-sky from cloud with MODIS algorithm theoretical basis document (MOD35)*, Cooperative Institute for Meteorological Satellite Studies, University of Wisconsin-Madison, NOAA/NESDIS, version 5.0, October 2006*
Allen, R.G., Tasumi, M., & Trezza, R. (2007). Satellite-based energy balance for mapping evapotranspiration with internalized calibration (METRIC) - Model. *Journal of Irrigation and Drainage Engineering-Asce, 133*, 380-394
Anderson, M.C., Kustas, W.P., Norman, J.M., Hain, C.R., Mecikalski, J.R., Schultz, L., Gonzalez-Dugo, M.P., Cammalleri, C., d'Urso, G., Pimstein, A., & Gao, F. (2011). Mapping daily evapotranspiration at field to continental scales using geostationary and polar orbiting satellite imagery. *Hydrology and Earth System Sciences, 15*, 223-239
Borbas, E.E., Hulley, G., Feltz, M., Knuteson, R., & Hook, S. (2018). The Combined ASTER MODIS Emissivity over Land (CAMEL) Part 1: Methodology and High Spectral Resolution Application. *Remote Sensing, 10*
Bulgin, C.E., Sembhi, H., Ghent, D., Remedios, J.J., & Merchant, C.J. (2014). Cloud-clearing techniques over land for land-surface temperature retrieval from the Advanced Along-Track Scanning Radiometer. *International Journal of Remote Sensing, 35*, 3594-3615
Feltz, M., Borbas, E., Knuteson, R., Hulley, G., & Hook, S. (2018). The Combined ASTER MODIS Emissivity over Land (CAMEL) Part 2: Uncertainty and Validation. *Remote Sensing, 10*
Fisher, J.B., Tu, K.P., & Baldocchi, D.D. (2008). Global estimates of the land-atmosphere water flux based on monthly AVHRR and ISLSCP-II data, validated at 16 FLUXNET sites. *Remote Sensing of Environment, 112*, 901-919
Hulley, G.C., & Hook, S.J. (2008). A new methodology for cloud detection and classification with ASTER data. *Geophysical Research Letters, 35*, L16812, doi: 16810.11029/12008gl034644

Irish, R.R., Barker, J.L., Goward, S.N., & Arvidson, T. (2006). Characterization of the Landsat-7 ETM+ automated cloud-cover assessment (ACCA) algorithm. *Photogrammetric Engineering and Remote Sensing, 72*, 1179-1188

Markham, B.L., & Barker, J.L. (1986). Landsat MSS & TM Post-Calibration Dynamic Ranges, Exoatmospheric Reflectances & At-Satellite Temperatures. In, *EOSAT Landsat Technical Notes, No. 1.*

Merchant, C.J., Embury, O., Roberts-Jones, J., Fiedler, E., Bulgin, C.E., Corlett, G.K., Good, S., McLaren, A., Rayner, N., Morak-Bozzo, S., & Donlon, C. (2014). Sea surface temperature datasets for climate applications from Phase 1 of the European Space Agency Climate Change Initiative (SST CCI). *Geoscience Data Journal, 1*, 179-191

Saunders, R.W., & Kriebel, K.T. (1988). An Improved Method for Detecting Clear Sky and Cloudy Radiances from Avhrr Data. *International Journal of Remote Sensing, 9*, 123-150